Landau and Ott scaling for the kinetic energy density in the low-T_c conventional superconductors Li_2Pd_3B and Nb

Mauro M. Doria and S. Salem-Sugui, Jr.
Instituto de Fisica, Universidade Federal do Rio de Janeiro, 21945-970 Rio de Janeiro, Brazil

P. Badica*
High Field Laboratory for Superconducting Materials, Institute for Materials Research, Tohoku University, 2-1-1 Katahira, Aoba-ku, Sendai, 980-8577 Japan

K. Togano
National Institute of Materials Science, Tsukuba, 1-2-1 Sengen, 305-0047 Japan
(Received 6 October 2005; revised manuscript received 19 April 2006; published 23 May 2006)

The scaling approach recently proposed by Landau and Ott for isothermal magnetization curves is extended to the average kinetic energy density of the condensate. Two low-T_c superconductors, Nb and Li_2Pd_3B are studied and their isothermal reversible magnetization is shown to display Landau and Ott scaling. Good agreement is obtained for the upper critical field $H_{c2}(T)$ determined from the Abrikosov approximation for the reversible region (standard linear extrapolation of the magnetization curve) and from the maximum of the kinetic energy curves. For the full range of data, which includes the irreversible region, the isothermal dMB/H^2 curves for Li_2Pd_3B show an impressive collapse into a single curve over the entire range of field measurements. The Nb isothermal dMB/H^2 curves exhibit the interesting feature of a constant and temperature independent minimum value.

DOI: 10.1103/PhysRevB.73.184524 PACS number(s): 74.25.Dw, 74.25.Op, 74.70.−b, 74.20.−z

Many methods have been used to determine the upper critical field $H_{c2}(T)$, some of them based on scaling laws which are expected to hold for the reversible magnetization.[1–3] Recently Landau and Ott applied successfully a new scaling method to many high-T_c reversible magnetization curves.[3–5] Several high-T_c materials[4] data sets, obtained using different experimental procedures, were shown by Landau and Ott to obey their predicted scaling. According to their scaling the H vs T phase diagram border is retrieved just from one single isothermal curve M vs H taken at some temperature T. M and H refer to the magnetization and the applied field, respectively. Their scaling has only been tested near T_c since the upper critical field is beyond the experimental range of observation for low temperature. In this paper we apply the Landau and Ott scaling to Li_2Pd_3B and Nb, which is the most studied of the low-T_c materials. We are motivated by the fact that for the low-T_c materials the temperature range covered is significantly larger as compared to the high-T_c materials.

The method of Landau and Ott,[3] inspired in the original Abrikosov's[6] theory, assumes a temperature independent Ginzburg-Landau parameter κ. The basic hypothesis is that the temperature dependence of the magnetic susceptibility $\chi(H,T) \equiv M(H,T)/H = \chi(h)$ is all contained in the reduced field $h = H/H_{c2}(T)$, that is, in the upper critical field at temperature T: $H_{c2}(T)$. From this it follows that

$$M(H,T) = H_{c2}(T) h \chi(h), \tag{1}$$

and the scaling relation connecting magnetization values at two different temperatures, T_0 and T, which is

$$M(H,T_0) = M(h_{c2}H,T)/h_{c2}, \tag{2}$$

$h_{c2} = H_{c2}(T)/H_{c2}(T_0)$. This relation implies that for all temperatures the $M(H)$ curves collapse into a single curve, once a suitable choice of the parameter $h_{c2}(T)$ is chosen for each curve. The collected set of scaling parameters $h_{c2}(T)$ plotted versus T leads to the determination of T_c. Thus the phase diagram borderline, H_{c2} vs T, follows from a single known value of $H_{c2}(T_0)$. Notice that the critical temperature T_c is not used as a fitting parameter in the method, instead it is obtained from extrapolation to zero field of the H_{c2} vs T scaling curve. A caveat is that all sources of magnetization other than the superconducting one must be removed before applying the Landau and Ott scaling.

In this paper we show that in the reversible region of large κ superconductors, the average kinetic energy density of the condensate is a universal function because its temperature dependence is in the reduced field h. The argument relies on the fact that the kinetic energy density of the condensate divided by the square of the applied field K/H^2 is a function of the magnetic susceptibility $\chi(h)$. Thus the kinetic energy density obeys a scaling law that directly follows from the Landau and Ott argument,

$$\frac{K}{H^2} = [1 + d\chi(h)]\chi(h). \tag{3}$$

The susceptibility determines the average kinetic energy density according to the above equation, though this direct connection is not explored here any further. The kinetic energy density can be directly read from the magnetization data. A few years ago some of us[7] have proposed a new way to plot M vs H isothermal magnetic data, through the dMB vs H

 ©2006 The American Physical Society

diagram, $B=(H+dM)$, B being the magnetic induction, and d being the demagnetization factor of the sample. Remarkably this quantity gives the average kinetic energy of the condensate for a sufficiently large κ superconductor,

$$K=-dMB, \tag{4}$$

as shown through the virial theorem.[7,8] This new plot unveils remarkable features present in the isothermal magnetization data. As discussed in Ref. 8 the isothermal plot dMB vs H vanishes in the Meissner region and also above the upper critical field H_{c2}, while a minimum (maximum value of the kinetic energy) is predicted to occur for a specific field H^*.[8] According to the Ginzburg-Landau theory this critical field, defined as H^*,[8] can be directly used to determine H_{c2}.

The recent discovery of superconductivity in the cubic perovskite Li_2Pd_3B (Ref. 10) has brought renewed interest in ternary borides containing alkaline and transition metals. Theoretical arguments indicate that strong electronic correlations[11] are important in this compound, though its low temperature specific heat behavior, namely its γ coefficient, is in agreement with a conventional Fermi liquid.[12] The Li_2Pd_3B cubic structure is composed by distorted Pd_6B octahedrons resembling the well known octahedral oxygen structure found in the high-t_c superconductors. Magnetic measurements have been performed in Li_2Pd_3B (Ref. 13) revealing a classic intermetallic compound. The coherence and London penetration lengths were found to be, $\xi=9.1$ nm and $\lambda=194$ nm, yielding a Ginzburg-Landau parameter $\kappa=21$. Properties of the phase diagram H vs T were obtained,[13] the Kramer curve $H_k(T)$ and the irreversibility line $H_{irr}(T)$, defined for vanishing critical current, were found to be linear.

For Nb, isothermal magnetization curves were obtained here for several temperature values using the same sample studied in Refs. 8 and 9, whose Ginzburg-Landau parameter is $\kappa=4$. According to Ref. 8 for $\kappa\geqslant 3$ the product dMB represents the average kinetic energy with precision better than 1%. Concerning the reversible (thermodynamic) region, new data points were added to the curves, leading to a better resolution than those described in Refs. 8 and 9. Points along these curves were obtained by increasing the field for fixed ΔH increments at the fixed, previously selected temperatures. In this way more detailed information about the reversible part of the H vs T diagram (used in the Landau and Ott analysis) is obtained. Magnetization data were always taken after cooling the sample in zero field. The measurements were done on a commercial Quantum Design SQUID magnetometer with 3 cm scans. We also consider here isothermal M vs H hysteresis data taken on an irreversible regime. This data is the same as the data of Refs. 8 and 9, here used for a different purpose, namely, the scaling analysis performed on the dMB vs H curves.

In this paper we find that the reversible magnetization of Li_2Pd_3B and of Nb obey Landau and Ott scaling. The original Landau and Ott proposal of scaling was for the reversible magnetization, but later they observed that scaling also applies below the irreversibility line for increasing fields.[5] The product dMB describes the average kinetic energy density of large κ superconductors, but just for the reversible region since the pinning interaction is not considered in this connection.[8] Similarly we apply scaling to the dMB curves of Li_2Pd_3B and Nb that are only partially in the reversible region. In the case of Li_2Pd_3B the scaling theory applied to dMB/H^2 produces an impressive collapse of all curves over the entire field range of field measurements. However, a similar collapse is not observed for Nb. This failure is blamed on the existence of a pronounced peak effect that the magnetization curves show near $H_{c2}(T)$, which is also present in the corresponding kinetic energy curves. Despite this absence of scaling, the curves of dBM/H^2 vs H for Nb show the same temperature independent maximum value, located just above H^*. This interesting new feature, only observed in the case of Nb, appears to be related to the critical magnetic field where full penetration in the sample takes place.

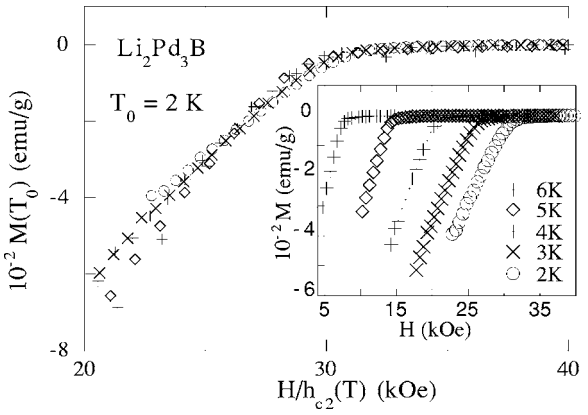

FIG. 1. The collapse of several Li_2Pd_3B isothermal reversible magnetization curves to the $T_0=2$ K curve, according to the Landau and Ott scaling. The inset shows the set of magnetization curves and their corresponding temperatures.

The demagnetization factor d used to obtain the quantity $K=dMB$ for the studied samples, is determined from the magnetization curves by assuming that $B=H+dM$ must vanish in the Meissner phase. For both compounds, Nb and Li_2Pd_3B, the removal of the background, namely, of the nonsuperconducting contribution to the magnetization, is found to be field dependent but not temperature dependent, as expected from Pauli paramagnetism.

The interest in the study of the reversible or thermodynamic part of the phase diagram stems from the high-T_c materials,[14,15] which exhibit a large and rich reversible region, opposite from that of the conventional low-T_c materials. High-T_c materials display an upward curvature in the irreversibility line, attributed, among others, to high-field diamagnetic fluctuations.[16–18] The Landau and Ott definition of the upper critical field $H_{c2}(T)$ brings a new switch to this controversial issue as it displays no upward curvature. We determine meaningful H_{c2} values for Li_2Pd_3B and Nb using the Landau and Ott scaling method on the reversible magnetization data.

Figure 1 shows the scaling analysis performed on the Li_2Pd_3B, according to Eq. (2). The collapse of the different temperature was achieved by searching suitable values of h_{c2}, following the choice of $T_0=2$ K. We observe that the

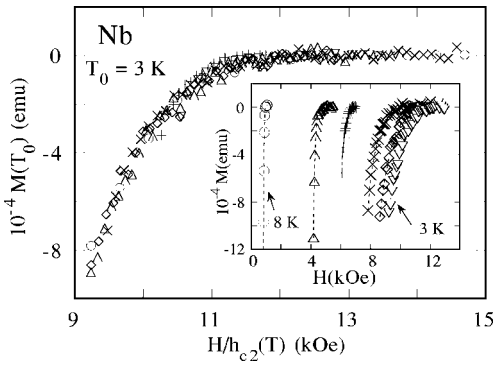

FIG. 2. The collapse of several Nb isothermal reversible magnetization curves to the $T_0=3$ K curve, according to the Landau and Ott scaling. The inset shows the set of magnetization curves and their corresponding temperatures.

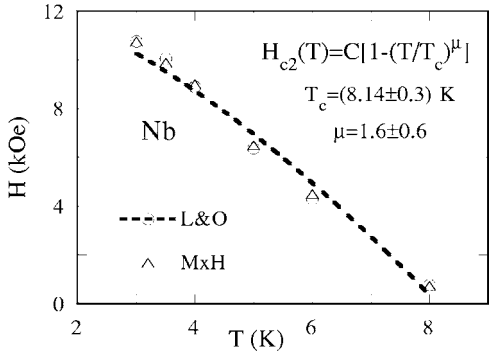

FIG. 4. Two $H_{c2}(T)$ curves for Nb are shown here, obtained directly from the M vs T reversible curves and from the Landau and Ott scaling method. From this last method one obtains the plotting exponent μ given here.

collapse only occurs for the reversible region, whose universal magnetization curve is shown in Fig. 1.

Figure 2 shows the same analysis of Fig. 1 performed on the Nb reversible magnetization data with the background magnetization already subtracted. The selected temperature for scaling is $T_0=3$ K. Concerning the scaling approach shown in Figs. 1 and 2, notice that for these low-T_c materials the isothermal M vs H curves are further apart from each other than the similar curves for high-T_c materials.[3–5]

The phase diagrams of Figs. 3 and 4 show $H_{c2}(T)$ values for temperatures much below T_c, away from the linear regime of the phase diagram. The fitting shown in Figs. 3 and 4 was obtained with $H_{c2}(T)=C[1-(T/T_c)^{\mu}]$, where $\mu=1.6$ for both studied samples and produced reasonable values for T_c. Figure 3 shows the phase diagram for Li_2Pd_3B. For Landau and Ott scaling $H_{c2}(T)$ is obtained from the h_{c2} values of the collapsed curve of Fig. 1, multiplied by $H_{c2}(T_0)$ obtained from the Abrikosov method. Figure 3 also displays the values of $H_{c2}(T)$ obtained from the linear extrapolation of the reversible region until $M=0$. Again, a remarkable agreement between both values of $H_{c2}(T)$ is found. The maximum of the kinetic energy H^* for Li_2Pd_3B was extracted from the dMB vs H curves and plotted in Fig. 3 and the constant ratio $H^*(T)/H_{c2}(T)\approx 0.61$ was found valid, thus nearly temperature independent in the studied range. The same temperature independent ratio was previously found to be 0.5 for our Nb sample.[8] To exemplify this technique, we also plot in Fig. 3 the values of $H_{c2}(T)$ obtained from the ratio $H_{c2}(T)/H^*(T) \equiv C$ where the constant $C=0.61$ is obtained from the ratio $H_{c2}(T=6\text{ K})/H^*(T=6\text{ K})$. As shown in Fig. 3 this is in good agreement with the Landau and Ott scaling and direct M vs H methods. The later method might be of particular interest when studying systems with higher values of $H_{c2}(0)$, since values of $H_{c2}(T)$ which may not be achieved experimentally can be estimated from the much lower values of H^*.

Figure 4 shows the phase diagram obtained for Nb. The obtained values of h are added to the value of $H_{c2}(T_0)$ determined from the Abrikosov method. Figure 4 also displays the values of $H_{c2}(T)$ obtained for the same curves presented in the inset of Fig. 2, but using the Abrikosov method. It is remarkable that the later values of $H_{c2}(T)$ for Nb virtually coincide with the values obtained from the scaling analysis of Fig. 2.

Figure 5 shows the scaling analysis for Li_2Pd_3B. The inset of Fig. 5 shows the 2 to 6 K M vs H curves extracted from Ref. 10. Their collapse into a single curve is impressive and extends over the entire range of field measurements, which

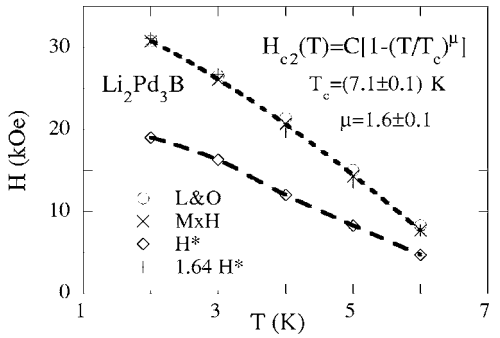

FIG. 3. Three $H_{c2}(T)$ curves for Li_2Pd_3B are shown here, obtained directly from the M vs T reversible curves, from the maximum in the kinetic energy curves and from the Landau and Ott scaling method. The curve $H^*(T)$ of the maximum kinetic energy is also shown here.

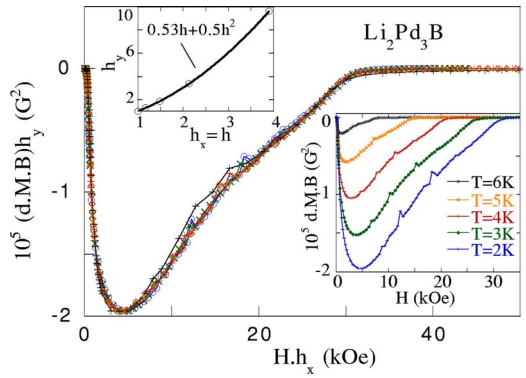

FIG. 5. (Color online) The collapse of several Li_2Pd_3B isothermal kinetic energy curves after scaling, following Eqs. (3) and (4). The lower inset shows the set of isothermal curves used in the main figure. The upper inset shows the scaling factors used to obtain the collapsed curve.

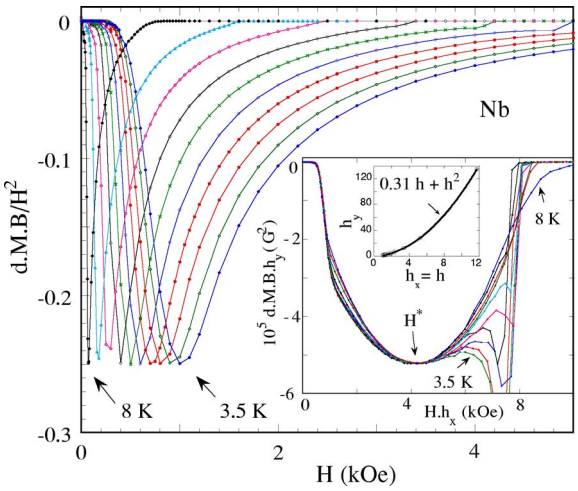

FIG. 6. (Color online) Isothermal kinetic energy curves dMB/H^2 vs H for Nb. The inset shows the collapse of the dMB vs H curves shown in the main figure after scaling following Eqs. (3) and (4). The inner inset shows the scaling factors used to obtain the collapsed curve.

includes the irreversible region. The universal curve shown in Fig. 5 was obtained after multiplying the y axis and the x axis of the dMB/H^2 curves (shown in the lower inset of this figure), by $h_y(T)$ and $h_x(T)$ where the values and the relation between $h_y(T)$ and $h_x(T)$ is presented in the upper inset of Fig. 5. It is worth mentioning that the relation between $h_y(T)$ and $h_x(T)$ does not spoil the h scaling as $h_x(T)$ virtually coincides with $h(T)$ obtained after applying the Landau and Ott scaling to the reversible magnetization curves. We stress that the relation between $h_y(T)$ and $h_x(T)$ is a fitting result found to be close to the prediction of Eq. (3).

Figure 6 shows the curves of the quantity dMB/H^2 for Nb, extracted from data obtained in Ref. 8. The lower inset of Fig. 6 shows the results of the kinetic energy scaling applied to the Nb curves. As mentioned in Fig. 5 above, the collapse shown in the inset of Fig. 6 covers the full region of field measurement, including the irreversible region. The inner inset displays the values of the scaling factors $h_y(T)$ and $h_x(T)$ used to obtain the lower inset figure. Notice that the relation between $h_y(T)$ and $h_x(T)$ is a best fitting choice similar to the prediction of Eq. (3). The arrow in the inset shows the position of H^*, and $h_x = H^*(T=3.5\ \mathrm{K})/H^*(T)$ and $h_y = K^*(3.5\ \mathrm{K})/K^*(T)$, where $K^* = K(H^*)$. As in Fig. 5, the relation between the scaling factors are in agreement with the scaling hypothesis. The values of $h_x(T)$ are in agreement with the scaling factor values $h(T)$ obtained after applying the Landau and Ott scaling to the reversible magnetization curves shown below. One sees in the lower inset of Fig. 6 that the collapsed kinetic energy curves mainly differ for fields above the minimum dMB point, namely for $H > H^*$. As previously mentioned this lack of scaling is related to the peak effect. An interesting result arises despite this lack of scaling. All dMB/H^2 curves exhibit the same minimum value which appears to be an intrinsic temperature independent effect. We mention that the field position of each minimum occurs very close to the field for which the sample is fully penetrated by the external field. This view is supported by the comparison between the dMB vs H plot and the corresponding M vs H curve. A similar plot for Li_2Pd_3B does not show a temperature independent maximum value, probably due to surface barriers and/or edge effects in this sample not considered in the present scaling approach developed for the bulk. One may observe that the curves of Fig. 6 suggest a new collapse of all dMB/H^2 curves by fine tuning x axis factors so as to adjust this secondary maximum to the same position. However, this proposal does not work due to the pronounced peak effect already present in our M vs H curves and enhanced in the dMB/H^2 curves.

In conclusion the reversible magnetization of Li_2Pd_3B and Nb are shown here to satisfy the Landau and Ott scaling as shown in Figs. 1 and 2. We also considered the isothermal magnetization measurements done in zero field cooled Li_2Pd_3B and Nb samples and used previous data obtained in increasing field data. For large κ superconductors we claim the universality of the average kinetic energy of the condensate based on the virial theorem, but Eqs. (3) and (4) were derived for the reversible regime. Zero field cooled isothermal magnetization data, casted as the product dMB/H^2 shows impressive scaling for Li_2Pd_3B but not for Nb. Interestingly the Nb isothermal dMB/H^2 curves exhibit a constant and temperature independent minimum value. The upper critical curve of the superconductor Li_2Pd_3B is obtained based on two new methods, namely, the Landau and Ott scaling and the maximum kinetic energy field. For comparison we have also studied Nb in order to display similar features in the low temperature compounds.

We would like to thank CNPq, FAPERJ, and one of us (M.M.D.) also thanks the Instituto do Milênio de Nanociências for financial support.

*Corresponding author. Also at National Institute of Materials Physics, P.O. Box MG-7, 077125 Bucharest, Romania. Email address: mmd@if.ufrj.br

[1] S. Ullah and A. T. Dorsey, Phys. Rev. Lett. **65**, 2066 (1990); Phys. Rev. B **44**, 262 (1991).
[2] Z. Hao and J. R. Clem, Phys. Rev. Lett. **67**, 2371 (1991).
[3] I. L. Landau and H. R. Ott, Phys. Rev. B **66**, 144506 (2002).
[4] I. L. Landau and H. R. Ott, Physica C **411**, 83 (2004).
[5] I. L. Landau and H. R. Ott, Phys. Rev. B **67**, 092505 (2003).
[6] A. Abrikosov, Zh. Eksp. Teor. Fiz. **32**, 1442 (1975) [Sov. Phys. JETP **5**, 1174 (1957)].
[7] M. M. Doria, J. E. Gubernatis, and D. Rainer, Phys. Rev. B **39**, 9573 (1989).
[8] M. M. Doria, S. Salem-Sugui, Jr., I. G. de Oliveira, L. Ghivelder, and E. H. Brandt, Phys. Rev. B **65**, 144509 (2002).
[9] S. Salem-Sugui Jr., Mark Friesen, A. D. Alvarenga, F. G. Gandra,

M. M. Doria, and O. F. Schilling, Phys. Rev. B **66**, 134521 (2002); Physica C **408–410**, 664 (2004).
[10] K. Togano, P. Badica, Y. Nakamori, S. Orimo, H. Takeya, and K. Hirata, Phys. Rev. Lett. **93**, 247004 (2004).
[11] M. Sardar and D. Sa, Physica C **411**, 120 (2004).
[12] H. Takeya, M. El Massalami, R. Rapp, and F. A. Chaves, Phys. Rev. B (to be published).
[13] P. Badica, T. Kondo, T. Kudo, Y. Nakamori, S. Orimo, and K. Togasno, Appl. Phys. Lett. **85**, 4433 (2004).
[14] J. G. Bednorz and K. A. Muller, Z. Phys. B: Condens. Matter **64**, 189 (1986).
[15] G. Blatter *et al.*, Rev. Mod. Phys. **66**, 1125 (1994).
[16] U. Welp, S. Fleshler, W. K. Kwok, R. A. Klemm, V. M. Vinokur, J. Downey, B. Veal, and G. W. Crabtree, Phys. Rev. Lett. **67**, 3180 (1991).
[17] L. N. Bulaevskii, M Ledvij, and V. G. Kogan, Phys. Rev. Lett. **68**, 3773 (1992).
[18] Z. Tesanovic, L. Xing, L. Bulaevskii, Q. Li, and M. Suenaga, Phys. Rev. Lett. **69**, 3563 (1992).